Design Overview of a Resonant Wing Actuation Mechanism for Application in Flapping Wing MAVs

C.T. Bolsman*, J.F.L. Goosen, and F. van Keulen
Delft University of Technology, Faculty of Mechanical, Maritime and Materials Engineering, Department of Precision and Microsystems Engineering, Mekelweg 2, 2628 CD Delft, The Netherlands

ABSTRACT

This paper deals with the design and analysis of the actuation mechanism for a four winged flapping wing MAV. The design is set up to exploit resonant properties, as exhibited by flying insects, to reduce the energy expenditure and to provide amplitude amplification. In order to achieve resonance a significantly flexible structure has to be incorporated into the design. The elastic structure used for the body of the MAV is a ring type structure. The ring is coupled to the wings by a compliant mechanical amplification mechanism which transforms and amplifies the ring deflection into the large wing root rotation. After initial sizing, the structures are analyzed by finite elements (eigenvalue and transient analysis). Based on the initial analysis, the structures are realized to be tested later.
The wings are first analyzed independent of the structure in order to tune wing hinge stiffness to efficiently generate lift, exploiting passive wing pitching. The wings are tuned by using a quasi-steady aerodynamic model. The tuned wings are tested to judge if manufactured wings reflect the predicted performance.
The ring-shaped thorax structure is combined with the wings to test resonant performance of the assembled structure. A test setup is built to quantify lift production. Lift is tested by suspending the prototype on a flexible beam and measuring changes in deflection when the model is actuated.

1 INTRODUCTION

The design and development of flapping-wing Micro Air Vehicles (MAVs) is inspired by flapping flight in nature. Larger insects and smaller birds achieve flight by comparable means, e.g., hawk moths and hummingbirds. In particular insects provide a source of inspiration from an engineering point of view due to the physiology of their thorax wing system. This system can be seen as a tuned resonator, see Greenewalt [1], which benefits the insect in several ways: resonant amplitude amplification of the wing sweeping motion, thereby allowing efficient lift production and second the reduction of energy expenditure required to accelerate and decelerate the wings, see Ellington [2]. Coupled to the wing sweeping motion is the wing pitching motion, which is achieved by passive means in insects, see Bergou *et al.* [3]. Especially the timing of wing pitching motion has a large influence on lift production. Consequently, in order to achieve efficient flight in flapping-wing MAVs, both effects, i.e. resonant wing sweeping and passive wing pitching, have to be integrated into the design requirements.
The scope of this paper is to provide an overview of the design decisions taken during the design and analysis and realization of the resonant wing actuation mechanism, which can be used for integration in a flapping wing MAV in a later stage. The intended size of this MAV is a 0.1m wingspan and it should be capable of slow moving and/or hovering flight, therefore a horizontal flapping plane is required. The process is split into three parts for simplicity, the actual design relies heavily on the interfaces between elements of the design. The first, is the mechanism that is to provide the coupling between the actuator and the wings via resonant coupling principles. The benefits of using these principles are given in Bolsman *et al.*[4] which discusses earlier design principles and possible mechanisms. Design choices and sizing are discussed, leading to a more detailed description of the realization process and choices therein. The second part is the design of the wings. The wings need to be aerodynamically efficient, this is accomplished by tuning wing stiffness to accomplish passive wing rotation. After the body and wings are individually analyzed, the complete structure is to be tested for performance in the third stage of testing and review.

2 RING-BASED STRUCTURES

To achieve a mechanical resonating structure energy storage is required. Typically this can be achieved via extension, compression, torsion and/or bending of an amount of material. The first two are ruled out by high mechanical loads involved. The drawback of the use of torsion is the usual need for support structures. Bending is the most attractive storage mode. An elegant form of the use of bending is to employ a ring type structure, which has self-contained vibration modes without the need for support structures. The main idea in this paper is to exploit the first bending mode to store elastic energy for the resonator. Another, more practical reason for

*Email address(es): contact_c.t.bolsman@tudelft.nl

using rings is that they provide adequate space on the inside to place a possible actuator. The ring and the corresponding bending mode is shown in Figure 1, with the attachment points for the wings indicated.

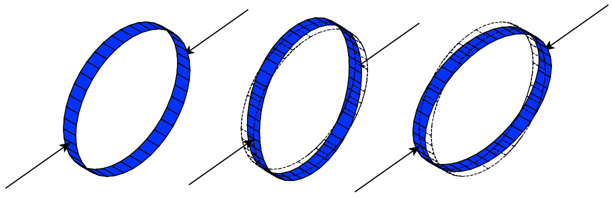

Figure 1: The deformation mode of the ring that is to be used, with the attachment points for the mechanical amplification mechanisms indicated by arrows

2.1 *Amplification mechanism*

In order to amplify and transform the linear movement of the edge of the ring to a large rotation of the wing root, a mechanical amplification mechanism is needed. In order to maintain the complaint nature of the structure and to ensure proper resonant properties, elastic hinges are used. A mechanism is proposed which allows for the connection of four wings in a symmetric setup, inspired by Cox *et al.*[5] and discussed in [6], see Figure 2. The mechanism couples

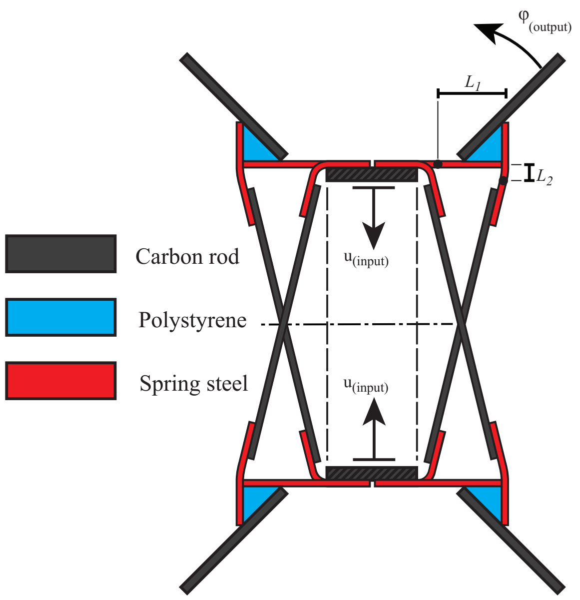

Figure 2: The compliant mechanism used to drive the wings

the linear motion of the ring, defined by u, to a large rotation at the wing root, defined by φ. This ratio of this coupling is defined as the transmission ratio by Wood [7] in analogy with the transmission ratio of a gearbox:

$$R = \frac{\varphi[\text{rad}]}{u[\text{m}]} \quad (1)$$

For design purposes only two lengths are of influence on this ratio, L_1 and L_2. These lengths are based on the effective centers of the compliant links, defined by Howell [8]. The angle of the strut has some influence but of lower order than other effects. L_2 should be kept small to ensure symmetric response around the center position, consequently the transmission ratio depends mostly on L_1. Due to the fact that both sides of the ring contribute to the input for the mechanism effective amplification ratio can be high. The relation between input and output is defined as:

$$\varphi = \arcsin\left(\frac{2u + L_2}{\sqrt{L_1^2 + L_2^2}}\right) - \arcsin\left(\frac{L_2}{\sqrt{L_1^2 + L_2^2}}\right) \quad (2)$$

In order to get an estimate for the initial sizing of the mechanism two requirements are of influence, the intended movement range of the wings and the stroke of the actuator, which limits the usable deflection of the ring. The movement is limited by using four wings in plane to $\sim 90°$ per wing. The chosen actuator has a maximum stroke of $\sim$ 6mm. The ring diameter, while not of large influence on the performance of the amplification mechanism is determined to be 28mm primarily to comfortably house the actuator. Using these values in Equation 1 leads to a required transmission ratio of $\sim$ 260rad/m. Equation 2 is used to obtain values for L_1 and L_2 which yield the required ratio. It must be noted that the value of L_2 is kept intentionally small at 0.5mm leading to a link length of 1mm to avoid buckling due to compression loading. L_1 is determined to be 4.5mm composed of half the length of the compliant link and the attachment point for the wing base.

2.2 *Modelling*

The structure is modelled using Finite Element (FE) analysis. The general dimensions are determined by the dimensions of the chosen actuator and by mechanism topology as determined above. Outside dimensions are determined by the size requirements which are in place for the MAV for which this actuation mechanism is developed. The first intention is to estimate ring stiffness required to reach the intended resonant frequency, which should lie in the range $\sim$ 25Hz to $\sim$ 40Hz based on intended vehicle mass. Masses of actuator, wings and amplification mechanism have been determined earlier and are used as is in the FE model. The ring stiffness has been determined by using an eigenfrequency analysis of the structure. The effects of the stiffness of the compliant links on the eigenfrequency of the structure is significantly lower than the influence of the ring stiffness.

It has to be noted that the choice of ring stiffness is not arbitrary but guided by available materials suitable for the construction of the ring. In this case two unidirectional carbon fiber rings are used to achieve the required value. In a later stage, dampers are added to the FE-model to simulate the effect of aerodynamic loads on the model. This damped model is used in a transient analysis of the system to evaluate the performance in large amplitude resonance. The models are actuated using a sinusoidal force with the frequency determined in the eigenvalue analysis. Actuation force is chosen such that the sweeping angle of the wings is close to required values, and the damping value of the dampers is such that the loads correspond to the aerodynamic loads. The minimum and maximum deflections, of the structure, reached during excitation in resonance are shown in Figure 3.

During the analysis, both the eigenvalue and transient, the

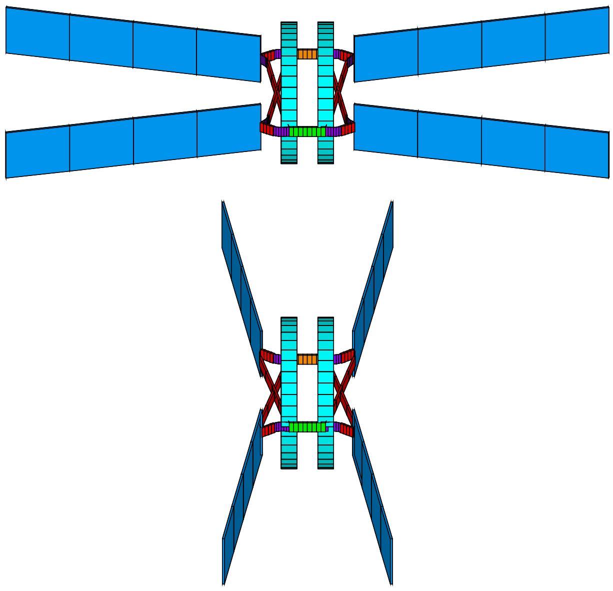

Figure 3: Minimum and maximum amplitude deflections of the structure in at resonance

effect of added mass, see Berman and Wang[9], due to the aerodynamics was not included. For the eigenvalue analysis this means that predicted frequencies are those for the structure operated in vacuum, and due to lower effective mass these frequencies will be higher than those in air. This is also true for the transient analysis, the non negligible value of the added mass can have large influence, which would effectively lower the predicted resonant frequency. The second property of interest is the stiffening behavior of the ring. Geometrically nonlinear effects induce stiffening, which causes the resonance frequency to increase when amplitudes become large.

2.3 *Realization*

The two rings, which function in parallel connected by a crossbar, are made from unidirectional carbon fiber strips, which are formed into a ring by glueing the ends together with an overlap. The strips have a 0.13mm x 3mm cross section. The ring diameter is determined mostly and actuator dimensions and is determined to be 30mm. The stress-state introduced into the ring by starting from a flat initial condition does not influence the eigenfrequencies of the ring, this is due to the fact that the stress-state is a pure bending moment and this does not lead to membrane stresses.

The mechanical amplification mechanism is made from carbon struts, 0.4mm x 2mm cross section and compliant hinges, which are made from 0.03mm thick, 2mm width spring steel. The wing attachment point is a triangular piece of polystyrene which is also used to attach the compliant hinges. Due to previous peeling problems in the glue connection between the spring steel and other parts, the need arose to secure these connections using nylon bond wires. The completed structure with both the two rings, the amplification mechanism and the actuator is shown in Figure 4.

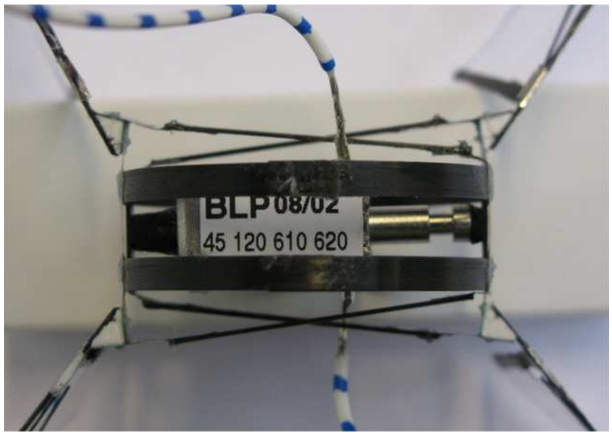

Figure 4: Top view of the structure showing the two rings and the amplification mechanism

The actuator used to test the prototypes for resonance is an off-the-shelf solenoid type actuator. This actuator is able to provide ample force but specific energy density is low. Generally solenoids actuate in one direction, which is not a problem when driving structures in resonance. The force-stroke curve of solenoids is not very suitable for efficient energy transfer to the structure. Maximum force is generated near the maximum of the stroke while the most efficient energy transfer, from actuator to structure, is achieved at the center of the stroke where velocities are highest and thus forces present can convey more power.

3 WINGS

The wings are based on a standard design commonly used in flapping wing MAVs. This design consists of a main stiff spar at the leading edge of the wing and two or more smaller spars which span a thin membrane. The design has been modified to include an flexible section which allows tuning of wing pitching stiffness, see Figure 5. The intention of this flexible section is to allow passive wing pitching, subject to inertial and aerodynamic loads, in order to achieve efficient lift production. The passive nature of wing pitching has been shown by Bergou *et al.*[3] for insects. The flexible section is in effect a hinge with tunable stiffness.

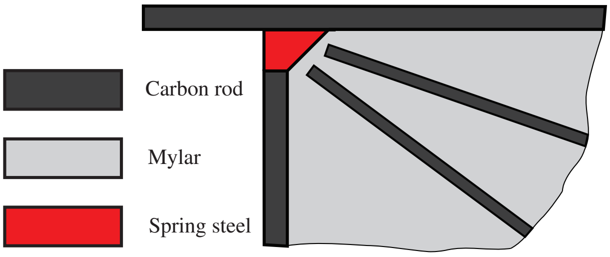

Figure 5: Representation of the wing base which indicates the position of the added flexible element to allow passive wing rotation

3.1 Modelling

The wing has been modelled by rigid bodies to account for wing inertia and morphological parameters, for example, the working axis of the hinge. The aerodynamic loads are added by making use of the quasi-steady model developed by Berman and Wang[9] and Pesavento and Wang [10]. Other quasi-steady models exist, Ellington [11] Sane and Dickinson [12], but current one is among the most recent. The aerodynamic parameters used are those for hawkmoths, which have wings of comparable size, intended flapping frequency and movement range. In this model it is assumed that all wing pitching is the result of the hinge rotation. Any deformation of the membrane, although adding to the effective wing pitching value is not taken into account. The second assumption is that all the stiffness is determined by the wing hinge, stiffness added by the membrane and geometrical effects are not taken into account. The wing planform used here is a very simple representation of a the shape of an hummingbird wing, the wing length is 50mm and the mean chord length is 16.75mm. Two models are created, the first is a reference model, which simulates the desired flapping motion with wing sweeping, pitching and heaving prescribed over time, following wing kinematics found in hawkmoths. The model has been checked to give the same output values as those by Berman and Wang[9] for equal input conditions, see [13]. The second model has prescribed sweeping and heaving but wing pitching is the resultant of the hinge stiffness and loads on the wing, both inertial and aerodynamic. The input flapping frequency for these models is determined by results from earlier experience with realized models and the FE model used to model the resonating structure. The wing pitching of the two models is compared over time and, subsequently, the wing hinge stiffness of the second model is tuned to minimize the difference between the two models. The hinge stiffness determined by this method is 2.38×10^{-4}Nm/rad.

3.2 Realization

The wings are realized using a combination of two carbon main rods (0.4mm x 1mm cross section) and mylar sheet (5×10^{-3}mm thickness). The mylar sheet is stiffened by two spars made from 0.28mm round carbon rod. The wing hinge is added by including a piece spring steel, 0.03mm thickness. The realized wing can be seen in Figure 6 on the left. The hinge in this model is constructed such that pitching stiffness of the wing corresponds to the value mentioned above. Before adding the wings to the prototype structure, they are tested in a simple test setup, which drives the wing sweeping in a sinusoidal motion with adjustable amplitude, see Figure 6 on the right. The pitching amplitude during the flapping motion is determined and reviewed by actuating the wing in this setup. An image taken of the actuated wing is shown in Figure 7, the picture direction is from the wing base to the tip, at the midpoint of the stroke, to be able to accurately visualize the mid-stroke pitching angle. This pitching angle has to correspond to desired values in order to create lift efficiently. After the wings are checked for performance they can be used on the prototype for measurements of the total system.

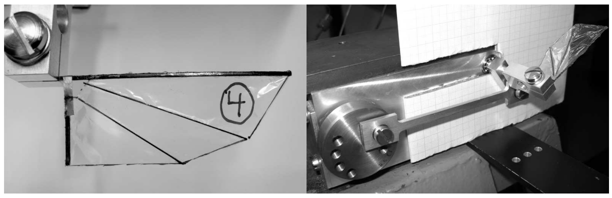

Figure 6: The completed wing showing the wing hinge structure (left) and the wing test setup (right)

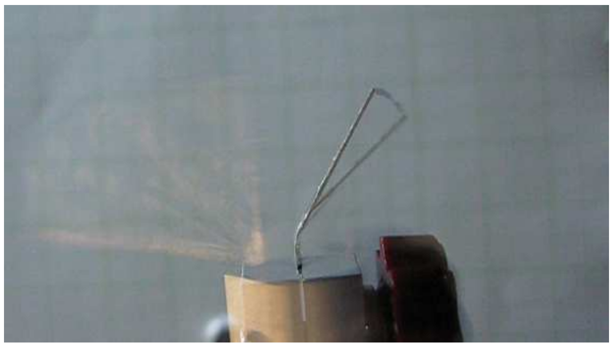

Figure 7: Mid-stroke pitching deflection of the wing, the direction shown is from the wing base to the wing tip along the main spar

4 Results

In order to test the structure a complete model has been built including the elastic base in the form of the rings, the amplification mechanism, the wings and the chosen actuator. The base structure and wings have been built as described. The wings are attached via the polystyrene triangular pieces shown in Figure 2, which provide a nice flat attachment base while also providing a means to influence the initial angle of the wings. Currently this angle is $\sim 45°$ to accommodate the predicted symmetric moving pattern. The structure is shown in Figure 8 to show distribution of the materials used. The actuator is not shown. The focus here lies on the performance of

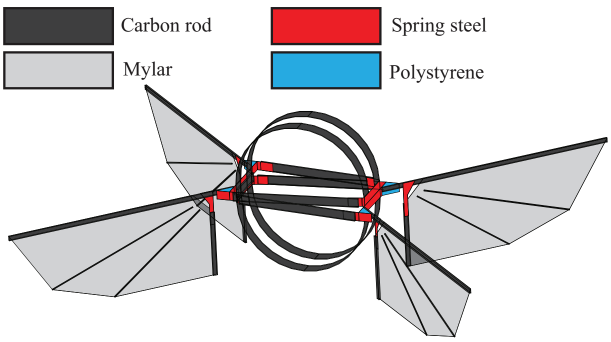

Figure 8: The total structure showing materials used

completed model. The realized model can be seen in Figure 9. The model is used to study two aspects: The wing kinematics and lift production. The first aspect is required to check if the wings provide movement following the required kinematics. Wing sweeping should have enough amplitude while wing pitching should follow kinematic patterns predicted and needed for efficient lift production. The second aspect is the generation of lift. This aspect is the pivotal property of the design.

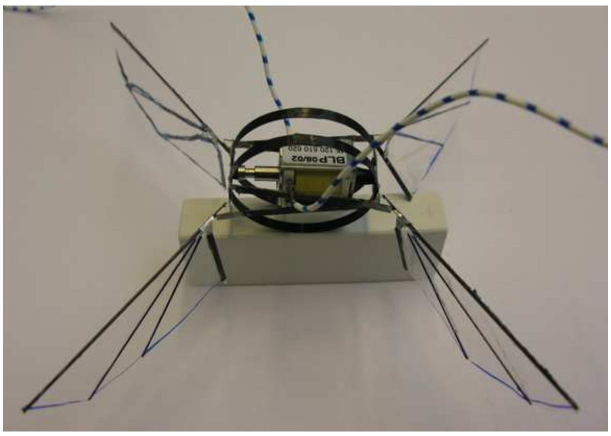

Figure 9: The total structure including: the rings, amplification mechanism, wings and the actuator

4.1 Test setups

Both aspects of the design, the generation of correct wing kinematics and the generation of lift, require the model to be driven at resonance. This is accomplished using a frequency generator and signal amplifier to drive the solenoid. Resonance is observed by visual means, augmented by a strobe light attached to a second frequency generator, which is driven at a different frequency to exploit the cyclic nature of the movement. The strobe light is also used to study the movement of the wings, for example, their pitch angle as a function of stroke angle.

The first measurement setup for the movement patterns: The movement of the structure is measured by suspending the model and using the strobe light to slow down the visible movement. This allows the visualization of the model in a range of motion from standstill, with the strobe light exactly at resonance frequency, or in a slow moving fashion when the strobe light is at a frequency near the resonance frequency. A camera is used to image the setup, still images are used to review the motion.

The second setup is designed to measure the lift produced by the prototype. This is accomplished by suspending the model from a simple cantilever beam and using deflection changes to measure lift production, see Figure 10. The beam is calibrated using known masses. Changes in beam deflection can be directly related to lift production.

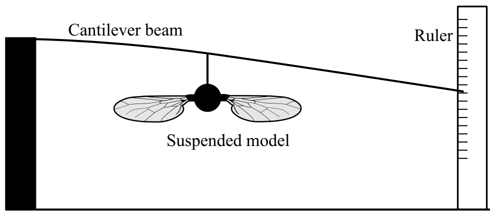

Figure 10: Test setup for measuring lift production of the suspended model

4.2 Kinematic patterns

The movement can be seen in Figure 11. It can be clearly seen that large amplitude wing sweeping is accomplished, comparable to the transient analysis, see Figure 3. An analysis of the pitching angle with respect to the sweeping angle shows that the wing pitching movement follows the kinematic pattern also found when testing a single wing in the wing testing setup. This pattern closely corresponds to the simple kinematic pattern commonly used to describe insect wing kinematics, i.e., sinusoidal wing sweeping and sinusoidal wing pitching with phase shift with respect to the sweeping.

4.3 Lift production

The amount of lift produced will very probably be below the weight of the prototype. The cantilever beam setup will be suitable for the force range from 0 to the weight of the structure. The setup has been calibrated to show a $1.25 \times 10^{-3} N/mm$ sensitivity. The prototype structure is actuated and driven in its resonant state, which is very close

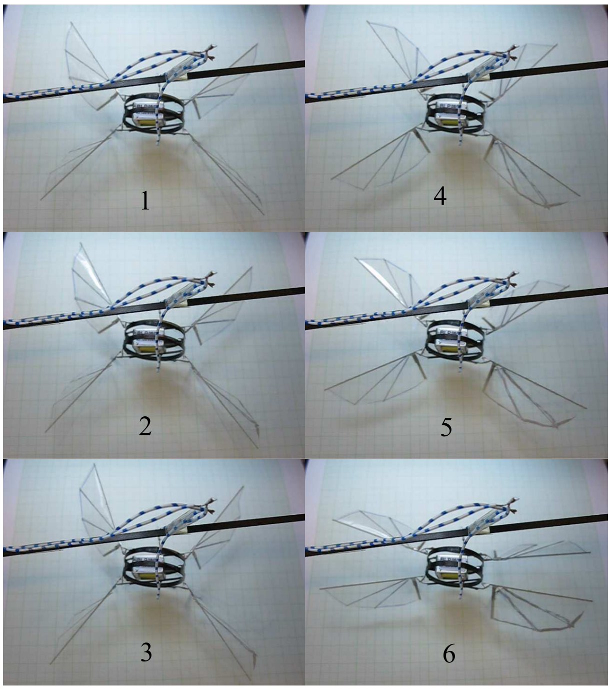

Figure 11: Sequence of pictures showing the the development of wing sweeping and pitching during one flapping cycle

to 27Hz for this model. The input to the solenoid is a sinusoidal signal with 12V amplitude. Care has to taken that the solenoid contracts for both the positive and negative part of the signal. Although some vibration of the cantilever is induced this is negligible compared to deflection changes induced by lift production. The prototype induces a $7mm$ deflection of the beam, corresponding to a lift production of $8.75 \times 10^{-3}N$ or approximately 0.9grams.

5 Conclusion and Outlook

The use of elastic structures to introduce and exploit resonant properties in the wing actuation mechanisms for flapping wing MAV application can be done in various ways. The method chosen in this work, the combination of a ring for energy storage with a compliant mechanism for movement amplification, meets the requirements set for this mechanism. The mechanism efficiently couples four wings to the elastic base, while retaining the completely compliant nature of the design. The resulting resonant frequency closely corresponds to predicted values. The wing sweeping motion is of sufficient amplitude for effective lift production. The wing pitching can be done by passive means using by introducing a flexible zone to traditional wing designs.
The lift measurements are below the values needed for liftoff. This is primarily due to the fact that the actuator currently used, has a low specific energy density and adds significantly to the active moving mass of the structure. Reduction of this mass will directly increase flapping frequency en thereby improve lift production. Another actuator technology with higher specific energy density will improve performance. Improvements are expected by changing the design of the wings. Changing the area and stiffness distribution of the wings may increase lift production. With these improvements implemented the ratio of lift to mass can be made more favorable towards liftoff of the structure and thereby allowing this wing actuation mechanism to be used in flapping wing MAV applications.

Acknowledgements

This work was supported by the DevClub and Casimir/NWO as part of the Atalanta project within DevLab.

References

[1] C. H. Greenewalt. The wings of insects and birds as mechanical oscillators. *Proceedings of the American Philosophical Society*, 104(6):605–611, December 1960.

[2] C.P. Ellington. The novel aerodynamics of insect flight: applications to micro-air vehicles. *The Journal of Experimental Biology*, 202(23):3439–3448, 1999.

[3] A.J. Bergou, S. Xu, and Z.J. Wang. Passive wing pitch reversal in insect flight. *Journal of Fluid Mechanics*, 591:321–337, 2007.

[4] C. T. Bolsman, J.F.L. Goosen, and F. van Keulen. Insect-inspired wing actuation structures based on ring-type resonators. *Active and Passive Smart Structures and Integrated Systems, SPIE, San Diego, USA, 2008*, 6928(1), 2008.

[5] A. Cox, D. Monopoli, D. Cveticanin, M. Goldfarb, and E. Garcia. The development of elastodynamic components for piezoelectrically actuated flapping micro-air vehicles. *Journal of Intelligent Material Systems and Structures*, 13:611–615, September 2002.

[6] C.T. Bolsman, J.F.L. Goosen, and F. van Keulen. Design and realization of resonant mechanisms for wing actuation in flapping wing micro air vehicles. In J.F. Silva Gomes and S.A. Mequid, editors, *Integrity, Reliability and Failure (IRF)*, Porto, Portugal, Juli 2009.

[7] R.J. Wood. Design, fabrication, and analysis of a 3DOF, 3cm flapping-wing MAV. In *IEEE/RSJ International Conference on Intelligent Robots and Systems, 2007. IROS 2007*, pages 1576–1581, 2007.

[8] L. L. Howell. *Compliant Mechanisms*. Wiley, 2001.

[9] G.J. Berman and Z.J. Wang. Energy-minimizing kinematics in hovering insect flight. *Journal of Fluid Mechanics*, 582:153–168, 2007.

[10] U. Pesavento and Z.J. Wang. Falling paper: Navier-stokes solutions, model of fluid forces, and center of mass elevation. *Physical Review Letters*, 93:14, 2004.

[11] C. P. Ellington. The aerodynamics of hovering insect flight. i. the quasi-steady analysis. *Royal Society of London Philosophical Transactions Series B*, 305:1–15, feb 1984.

[12] S. P. Sane and M. H. Dickinson. The aerodynamic effects of wing rotation and a revised quasi-steadi model of flapping flight. *The Journal of Experimental Biology*, 205:1087–1096, 2002.

[13] C.T. Bolsman, J.F.L. Goosen, and F. van Keulen. Compliant structure design for reproducing insect wing kinematics in MAVs. In *proceedings of IFASD conference (to Appear)*, Seattle, Washington, USA, June 2009.